PROCEEDINGS, 50th Workshop on Geothermal Reservoir Engineering
Stanford University, Stanford, California, February 10-12, 2025
SGP-TR-229

Curie point depth analysis for assessment of supercritical carbon recycle CO2 geothermal power generation

Yasukuni Okubo, Shoichi Yamano, Shunsuke Akazawa, Kazumi Osato, Amane Terai

Geothermal Energy Research & Development Co., LTD., 22-4, Shinkawa 1-chome, Chuo-ku, Tokyo, Japan

yasu-okubo@jcom.home.ne.jp

Keywords: Curie point, Japanese Islands, earthquake, geothermal

ABSTRACT

Since 2011, the Japanese government has begun a policy to enhance renewable energy. This includes a project of supercritical carbon recycle CO2 geothermal power generation. Okubo et al. (2023) calculated Curie point depths (CPDs) of Japan using the method developed by Bouligand et al. (2009) for a new type of geothermal resources assessment. The result was compared with drillhole data. The comparison indicates that the CPDs represent reginal geothermal structures but fail to delineate local anomalies due to the average effect.

Using Leapfrog Geothermal modeling software, we compiled CPDs and drillhole data in the Hachimantai geothermal field and made a 3-D geothermal structural model covering no drillhole data areas.

Cross section of the 3-D geothermal model crossing Akita-Komagatake and Iwate volcano shows that the isotherms rise from west to east. This also shows local geothermal anomalies around the Matsukawa geothermal power plant (GP). The Kakkonda GP is located on the slope of the isotherm rise.

Gravity anomaly map shows that the Kakkonda GP is on the slope of a gravity hill and that the Matsukawa GP is at the top of a gravity hill. We interpreted that the area around the Kakkonda GP is highly fractured and that the area around the Matsukawa GP is less fractured.

ScCO2 power generation requires high temperatures and few fractures. We interpret that the area around Matsukawa GP is suitable for ScCO2 power generation.

1. INTRODUCTION

Since 2011, Japan has launched a policy to increase carbon-free energy, including geothermal energy. The installed capacity of geothermal power generation in Japan is about 550 MW and has not grown much for the last quarter century. The main reasons are conflicts with a hot spring spar or “Onsen”, which is a major traditional tourism industry in Japan, and restrictions on development in national parks. Now, the Japanese government has addressed these issues.

Development of new technologies is another policy. A geothermal power generation using supercritical CO2 (ScCO2) is one of these new technologies. This concept was proposed by Brown (2000) based on the experience of the very extensive Hot Dry Rock (HDR) research conducted by Los Alamos National Laboratory at Fenton Hill. To extract energy from dry rocks at depth, enhanced geothermal systems (EGS) are currently being developed.

As a result of various drilling surveys in Japan, many geothermal areas have been discovered, including many areas where high temperatures have been confirmed at depth but no signs of hot water have been found. These areas are thought to be hot dry rock areas. Japan Organization for Metals and Energy Security (JOGMEC) launched the project of geothermal system using ScCO2 in 2021 in order to develop such hot dry rock areas. This is a technology to generate electricity using ScCO2 instead of water.

Towards the goal, JOGMEC is conducting three subjects over a five-year period from 2021 to establish basic technologies: I. overall system design, II. reservoir creation using ScCO2 as fracturing fluid, and III. CO2 flow and geochemical reaction in a geothermal reservoir. In the USA, a map of geothermal energy potential of hot dry rock across the USA (National Renewable Energy Laboratory, 2018) has been published. Following the achievement, in the overall system design, in order to reveal the geothermal structure of the Japanese islands and to estimate the potential for ScCO2 geothermal power generation, we conducted Curie point depth analysis.

Various methods have been proposed to calculate Curie point depth (CPD) from a spectral analysis of the magnetic anomaly. CPD is the depth at which crustal temperatures reach the Curie point of the dominant magnetic minerals. Magnetite is the most prevalent magnetic mineral, in terms of susceptibility and quantity, and has a Curie point of 580 ˚C. Therefore, CPD is often interpreted as the depth to the 580 ˚C isotherm. Okubo et al. (1989, 1991) used the method of Spector and Grant (1970) to calculate CDPs of the Japanese Islands. The results show that the CPDs range 6-10 km in volcanic regions and 10 km or deeper in non-volcanic regions. They were compiled and published as the CPD map of the Japanese Islands, a handwritten contour diagram (Okubo et al., 1989).

Maus and Dimri (1996) hypothesized that the magnetic material has a fractal distribution, and developed an equation of the power spectrum of magnetic anomalies. Based on the equation Bouligand et al. (2009) developed a new CPD analysis and applied it to the western United States.

Using East/Southeast Asia magnetic anomaly map (3rd edition) at 2-minute intervals (Ishihara and Uchida, 2021) (we call it “IshiharaV3” hereafter), Okubo et al (2023) calculated CPDs of the Japanese Islands by the method of Bouligand et al. (2009). The results range 6-9 km deep in volcanic areas and are deeper than 9 km in non-volcanic areas. The results were concordant with the previous study by Okubo et al. (1989) indicating that CPD represents a regional geothermal structure.

The drillhole database compiled by JOGMEC shows many measurements of depth-to-temperature (DtT) curves in volcanic areas. In this paper, taking the Hachimantai geothermal field (GF) in the Tohoku arc as an example, we compile the results of CPD analysis and the drillhole data in order to construct a 3-D geothermal structural model and discuss the potential of ScCO2 geothermal system.

2. TECTONIC CONTEXT OF JAPANESE ISLANDS

The geothermal structure of the Japanese Islands where four tectonic plates converge is most complex in the earth (Figure 1). As the Japanese Islands is a typical island arc at the margin of continent where oceanic plates have been subducting under overriding crust, the geothermal structure depends not only on the factors of continent but also on oceanic plate and its interaction with the overriding crust and mantle.

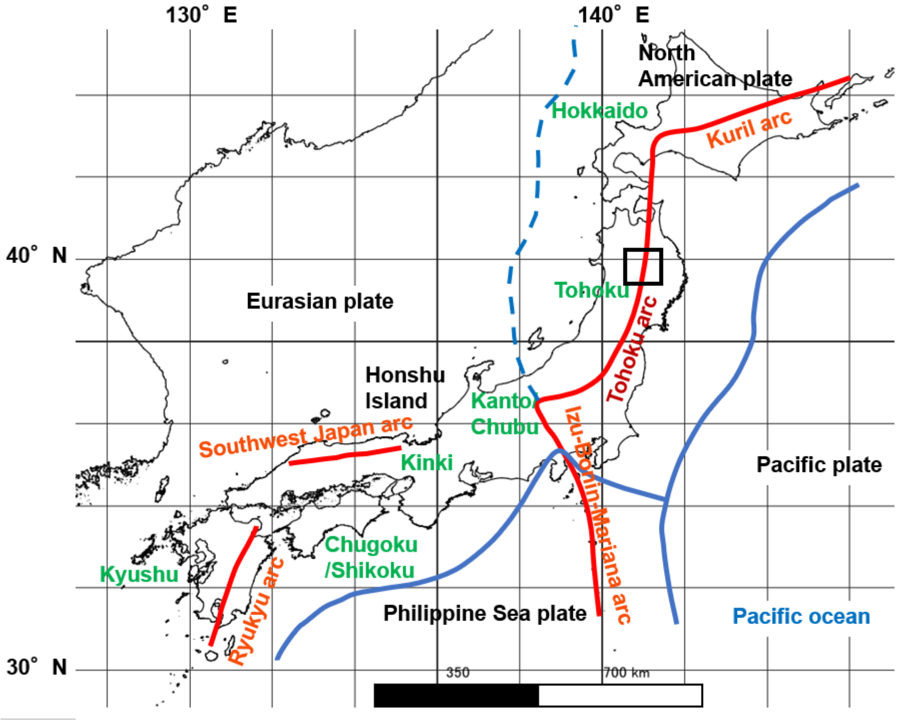

Figure 1: Tectonic context of Japanese Islands. Red lines are volcanic fronts. Blue lines are plate boundaries. Black square is the location the Hachimantai GF.

In northeast Japan, the Pacific plate has been subducting west-northwestward beneath the land area, which lies on the southernmost portion of the North American plate (or Okhotsk plate). In southwest Japan, the Philippine Sea plate has been subducting northwestward beneath the land area. This tectonically complex situation causes high volcanic and seismic activities.

The Tohoku arc lies west Hokkaido and the northern part of Honshu Island trending north-south. The geothermal structure of the Tohoku arc has been characterized on the basis of available geothermal data. The geothermal data reveal high vertical geothermal gradients in the back arc and low gradients in the forearc (e.g., Hasebe et al., 1970).

3 CPD Analysis method applied to magnetic data

The theoretical power spectrum due to a slab of self-similar magnetization distribution is given by Maus and Dimri (1996). The power spectrum depends on three parameters, the top depth of the magnetized layer (Zt), the thickness of the magnetized layer (Dz), and the fractal coefficient β. CPD is simply calculated from Zt and Dz by the following formula.

$$CPD = Zt + Dz$$

We used the Bayesian framework to determine the three parameters simultaneously. The algorithms were implemented within PyCurious by Python, an open-source Python package.

The map of CPD of the Japanese Islands was published by Akazawa et al. (in press). The map is by the method of Bouligand et. al. (2009) using the data of IshiharaV3 with a window size of 50 km by shifting 5 km both in longitude and latitude direction. The map shows reginal geothermal structures in Japan.

4 COMPARISON BETWEEN CPDS AND DRILLHOLE DATA IN HACHIMANTAI GF

The study area, the Hachimantai GF is located in the Tohoku arc. Volcanoes of Akita-Yakeyama, Hachimantai, Iwate volcano, and Akita-Komagatake are distributed there. In addition, the Kakkonda geothermal power plant (GP) (8.0MW), the Matsukawa GP (2.3MW), the Matsuo-Hachimantai GP (0.7MW), the Onuma GP (1.0MW), and the Sumikawa GP (5.0MW) are in operation.

The drillhole database compiled by JOGMEC shows a number of measurements of DtT curves of drillholes in volcanic areas. The data provide local observed geothermal structure of the Hachimantai GF. Figure 2 shows the locations of volcanoes, geothermal power plants and drillholes in the study area.

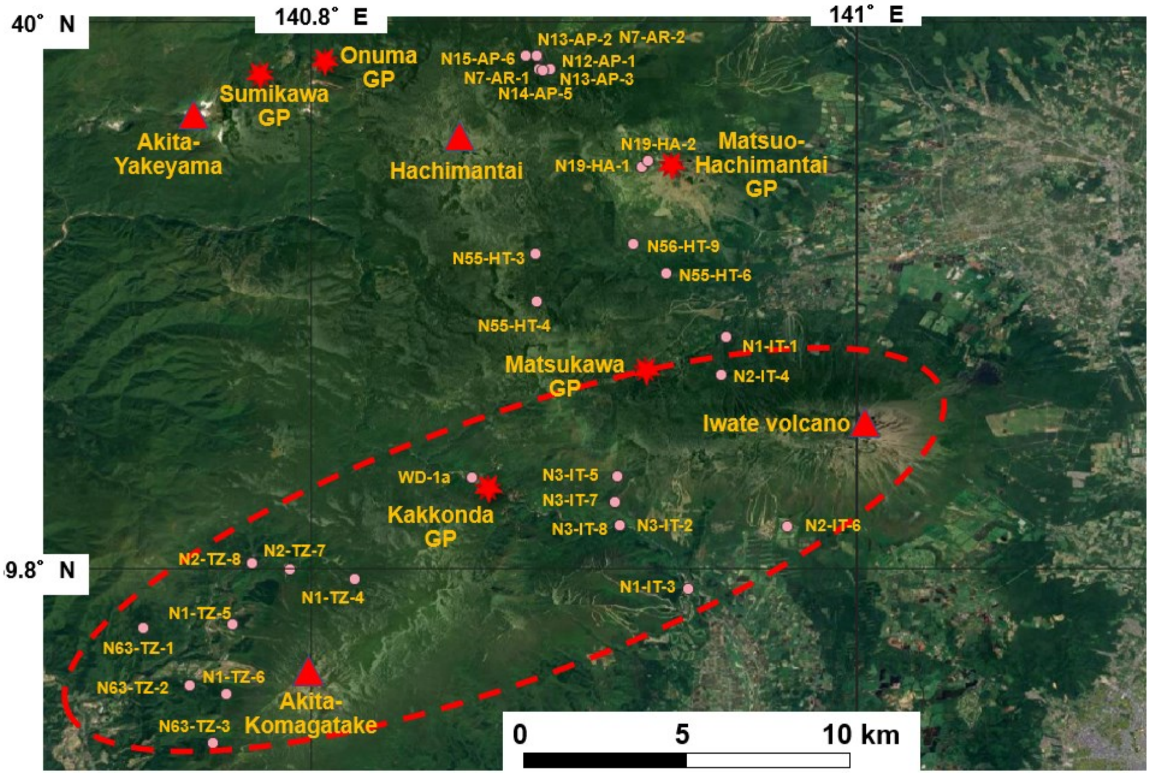

Figure 2: Locations of volcanoes, geothermal power plants and drillholes in the Hachimantai GF. Red broken circle indicates the area of Figure 3.

The temperatures in the JOGMEC database are ones at the final standing time in the recovery test and static temperatures estimated from the results of the recovery test. As the deeper the underground, the less the influence of the surface water is and the less the convection of the fluid is, the DtT curves deeper than the sea level must represent the heat conduction type geothermal gradient. Therefore, the DtT curves deeper than the sea level must represent the heat conduction type geothermal gradient rather than the shallow DtT curves.

The temperature distribution in the continental crust and lithosphere is governed mainly by the conductive heat loss to the surface that is generated internally by the decay of radioactive elements in the rocks and heat that flows upward from the subcontinental mantle. Heat flow in the continents can be partly attributed to the heat production from the radioactive elements of uranium, thorium, and potassium in the continental crust (Turcotte and Schubert, 1982). Prediction of the temperature with depth should be taken into consideration of the heat production. If radioactive elements are uniformly distributed in the crust, the geothermal conductivity is constant and heat flow is conductive, the geothermal gradient gradually decreases with increasing depth due to heat generation of the radioactive elements. Here we discuss the geothermal structure of the bottom of hole and the depths shallower than several km below the surface. Then we assume that the effect of heat generation due to the radioactive elements in that depth range can be neglected. Based on the assumption, geothermal gradients were obtained. Table 1 shows the geothermal gradient obtained by the least squares method using DtT data of the Hachimantai GF deeper than the sea level.

Table 1: Data of drillholes used and their geothermal gradients obtained by the least squares method using DtT data deeper than the sea level. Geothermal gradient of WD-1a marked with * is the average geothermal gradient from the wellhead to the bottom.

Name of Drillhole	Latitude	Longitude	Elevation(m)	Botom Elevation (mBSL)	Bottom Temperature (°C)	Geothermal Gradient (K/m)	
N1-IT-1	39.884685	140.952074	731	-267	133.8	0.169738179	
N1-IT-2	39.815736	140.913196	488	-507	219.9	0.18354747	
N1-IT-3	39.792405	140.938005	462	-538	113.5	0.133376024	
N2-IT-4	39.870678	140.950403	845	-355	176.8	0.173749035	
N2-IT-5	39.833617	140.912111	950	-251	283.5	0.214404454	
N2-IT-6	39.815166	140.974415	707	-493	124.4	0.097613926	
N3-IT-7	39.824444	140.911529	955	-535	278.6	0.208660187	
N3-IT-8	39.815695	140.913204	488	-1212	316.6	0.156619237	
N55-HT-3	39.915052	140.882242	1152	-348	218	0.092207283	
N55-HT-4	39.8975554	140.882698	1160	-190	148.5	0.091052632	
N55-HT-6	39.9081549	140.929956	740	-260	135.3	0.117216117	
N56-HT-9	39.918975	140.918131	873	-127	143.7	0.121703297	
N19-HA-1	39.9470215	140.92097	996	-483.651968	287	0.228208772	
N19-HA-2	39.9493564	140.923394	996	-472.821884	265.3	0.186328156	
N7-AR-1	39.9829426	140.883359	1188.9	-440.083478	269	0.181134425	
N7-AR-2	39.98751	140.88311	1166.4	-440.083478	269	0.224106535	
N12-AP-1	39.9879448	140.882973	1083.9	-400.972308	264.8	0.290893235	
N13-AP-2	39.9877552	140.882871	1165.1	-486.438276	260.4	0.16820114	
N13-AP-3	39.9827653	140.887425	1165.1	-747.535	342.3	0.222664085	
N14-AP-5	39.9822926	140.885059	1189	-705.325806	336.5	0.190897678	
N15-AP-6	39.9879961	140.878699	1165.1	-319.772308	264.8	0.314966434	
N63-TZ-1	39.778332	140.738327	590	-410	90.1	0.072354752	
N63-TZ-2	39.756943	140.75528	480	-520	94.4	0.082670537	
N63-TZ-3	39.735832	140.763885	620	-380	62.5	0.067441296	
N1-TZ-4	39.796112	140.815826	915	-85.5	236.1	0.064980519	
N1-TZ-5	39.779446	140.771118	665	-837	143.7	0.086454795	
N1-TZ-6	39.754166	140.76889	710	-791	128.8	0.078289946	
N2-TZ-7	39.799721	140.792221	760	-740	146.8	0.072922333	
N2-TZ-8	39.801945	140.778336	630	-772.9045455	140.1	0.077861152	
WD-1a	39.833057	140.858887	680	-3469.34	500.8	0.283751998	*

By assuming that the geothermal gradients are constant from the bottom of hole to the deeper part, we can make a virtual DtT curve below the bottom of hole. To compare the Curie point depths with drillhole data, we calculated the CPD from the virtual DtT curve. We call it "virtual CPD (vCPD)".

Figure 3 is a west northwest – east southeast cross section of vCPD and CPD across the Kakkonda and the Matsukawa GPs. CPD is 6.8 km below sea level west of Akita-Komagatake and gradually becomes shallower toward to the east, reaching 4.6 km near Iwate volcano. On the east side beyond Iwate volcano CPD becomes deeper. On the other hand, vCPDs range 5.9 – 7.1 km in the west side which are concordant with CPDs. vCPDs around the Matsukawa GP, however, show local high anomalies ranging 1.6-2.9 km below sea level which are much shallower than CDPs.

Consequently, CPDs miss to extract the local high anomalies. As the magnetic data for the CPD analysis performed here is the data with window size of 50 km, the CPD must correspond to the average value of the 50 km square area (Okubo et al. 2023).

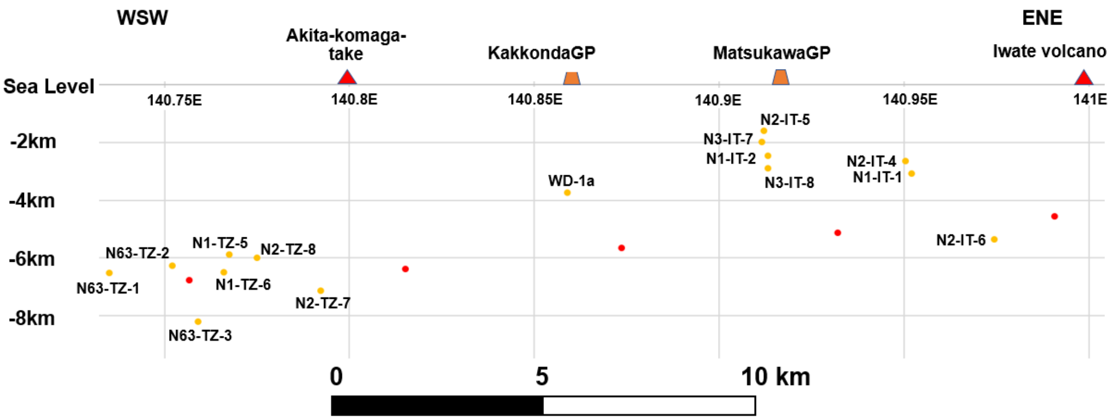

Figure 3: West southwest - east northeast cross section of CPDs (red dots) and vCPDs (yellow dots) across Akita-Komagatake, the Kakkonda GP, the Matsukawa GP and Iwate volcano. Location is in Figure 2.

5. COMPILATIO OF CPDS AND DRILLHOLE DATA AND DISCUSSIONS

Here, we estimate the geothermal structure at depth and evaluate the potential of ScCO2 geothermal power generation by compilation of CPDs and drillhole data.

Leapfrog Geothermal modeling software has been developed to model and visualizes geothermal systems in three dimensions. The models are based on mathematical interpolation functions, and this provides a grid-free representation of the geological structure and numerical quantities such as temperature and pressure (Newson et al., 2012).

As shown in Figure 3, drillhole data can extract local high temperature areas. However, the distribution is uneven and there are almost no data areas. In this approach, the initial step in integrating temperature model into Leapfrog Geothermal is to assign dummy drillholes obtained by CPDs in order to cover the areas where there is no drillhole data. By assuming that the Curie point to be 580°C at the Curie point depth, 15°C at the surface and that the geothermal gradient is constant, we can make a dummy DtT curve.

DtT of drillhole are restricted at shallow parts ranging about 1000 m – 4000 m (Table 1). Then we extrapolate the DtT curve below the bottom of hole by assuming that the geothermal gradients shown in Table 1 are constant from the bottom of hole to the deeper part.

The next is to integrate the extrapolated DtT curves and the dummy DtT curves calculated from the CPDs. In this way, we obtain a 3-D geothermal structural model for the entire Hachimantai GF. Figure 4 shows the contour of depth reaching supercritical temperature of water, 347°C.

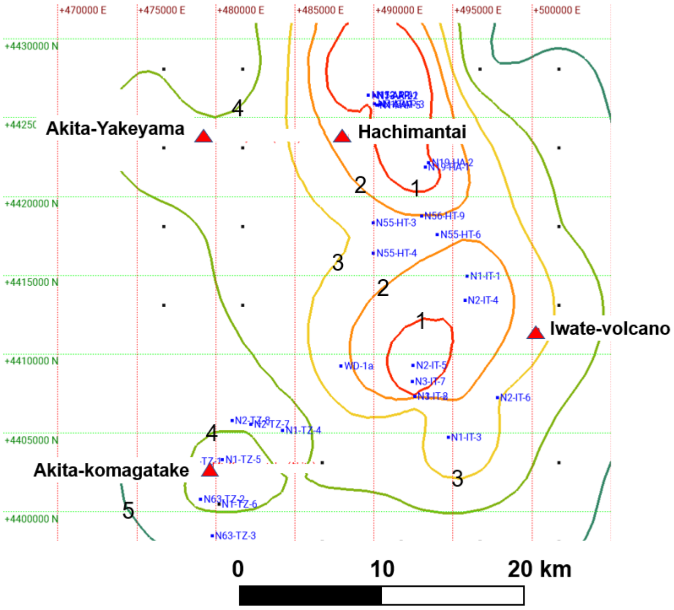

Figure 4: Contour of depth from the ground surface reaching supercritical temperature of water, 347°C. Contour interval is 1 km. Black dots denote locations of the dummy drillholes by CPD analysis. Blue dots are locations of drillholes from the JOGMEC database.

Figure 5 shows cross section of the geothermal structural model across Akita-Komagatake and Iwate volcano. This shows local geothermal anomalies around the Matsukawa GP. The 374°C isotherm is at a shallow depth of about 1 km below sea level. Around Akita-Komagatake, the 374°C isotherm is at a deeper depth of about 4 km. The isotherms rise from west to east. The Kakkonda GP is located on the slope of the isotherm rise.

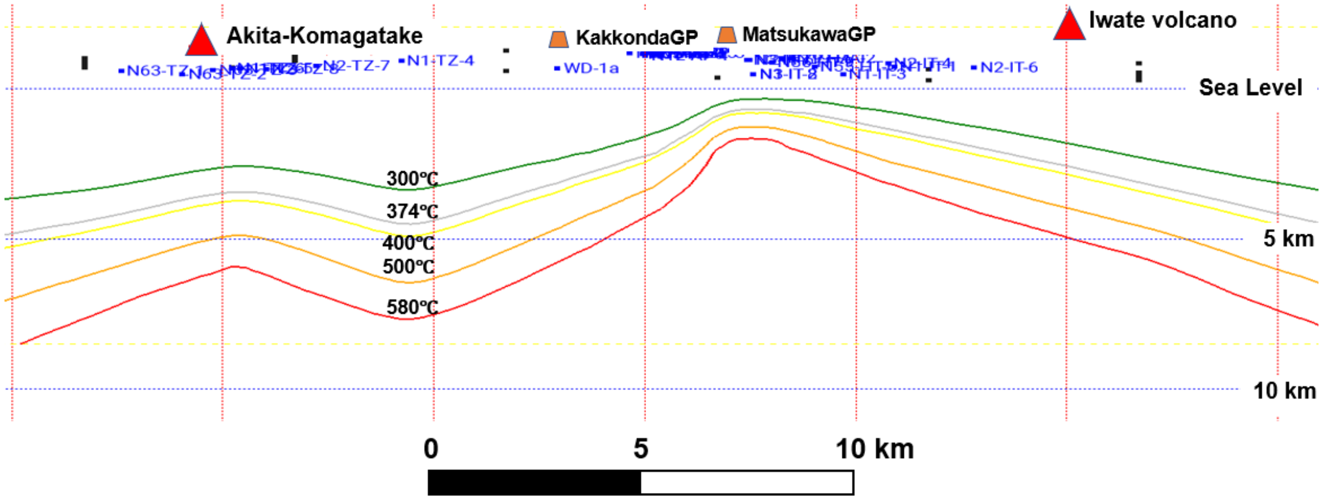

Figure 5: Cross section of geothermal structure across Akita-Komagatake and Iwate volcano.

ScCO2 has a much lower viscosity to density ratio than water which suggests it could be superior for reservoirs with lower permeability (Taylor, 2014). Here, we assume a two-layer model consisting of a sedimentary layer and an underlying geological basement. The sedimentary layer could be relatively permeable and the geological basement could have lower permeability. Since the gravity data is a good reference about the depth of the geological basement, we interpret the gravity data.

The gravity map published by Geological Survey of Japan, AIST (2013) over the Hachimantai GF shows variation of high and low gravity anomalies with an amplitude of about 15 mGal and a wavelength of about 5 km. The Matsukawa geothermal power plant is at the top of a gravity hill and the Kakkonda GP is on the slope of the gravity hill.

We interpreted that the gravity high, at which the Matsukawa GP is located, represents less fractured zone and that the area of gravity slope, at which the Kakkonda GP is located, is a highly fractured zone associated by the intrusion. Consequently, there are hydrothermal convections in the fractured zone around the Kakkonda GP.

Power generation using supercritical geothermal water requires high temperatures and the presence of a reservoir, while ScCO2 power generation requires that CO2 does not leak, so high temperatures and few fractures are required. The model in Figure 5 shows that the area around Kakkonda GP is suitable for power generation using supercritical geothermal water, and the area around Matsukawa GP is suitable for ScCO2 power generation.

The above is a preliminary interpretation. In the future, we will fully interpret a geothermal structural model integrating the CPDs, the drillhole data, the data by gravity analysis and the data from geophysical and geochemical surveys.

6. CONCLUSIONS

Comparison between CPDs by Okubo et al. (2023) and drillhole data in the Hachimantai GF shows that CPDs miss to extract the local high anomalies. The reason is that the CPD corresponds to the average value of the 50 km square area which is the window size for CPD analysis.

By integrating the extrapolated DtT curves of drillholes and the dummy DtT curves calculated from the CPD, we obtain a 3-D geothermal structural model for the entire Hachimantai GF.

Cross section of the 3-D structural model crossing Akita-Komagatake and Iwate volcano shows that the isotherms rise from west to east. This also shows local geothermal anomalies around the Matsukawa GP. The Kakkonda GP is located on the slope of the isotherm rise.

The gravity map shows that the Kakkonda GP is on the slope of a gravity hill and that the Matsukawa GP is at the top of a gravity hill. We interpreted that the area around the Kakkonda GP is a highly fractured zone and that the area around the Matsukawa GP is less fractured.

ScCO2 power generation requires that CO2 does not leak, so high temperatures and few fractures are required. We interpret that the area around Matsukawa GP is suitable for ScCO2 power generation.

ACKNOWLEGEMENT

This work is supported by a fund for the project “Carbon recycle CO2 geothermal power generation technology” from the Japan Organization for Metals and Energy Security (JOGMEC).

REFERENCES

Akazawa, S., Okubo, Y., Yamano, S., Osato, K. and Terai, A. (in press) Curie point depth map in Japan - Assessment in the Hatchobaru Geothermal Area-, Journal of the Geothermal Research Society of Japan.

Bouligand, C., Glen, J. M. G. and Blakely, R. J. (2009) Mapping Curie temperature depth in the western United States with a fractal model for crustal magnetization Claire, Journal of Geophysical Research, 114, B11104, doi:10.1029/2009JB006494.

Geological Survey of Japan, AIST (2013) Gravity Data Base of Japan, DVD Edition.

Hasebe, K., Fujii, N. and Uyeda, S. (1970) Thermal processes under island arcs, Tectonophysics, 10, 335-355.

Ishihara, T. and Uchida, T. (2021) Magnetic Anomaly Map of East and Southeast Asia, Revised Version (3rd Edition), Digital Geoscience Map P-3 Revised, Geological Survey of Japan.

Japan Oil, Gas and Metals National Corporation (JOGMEC) Geothermal database system, https://geothermal-db-web.jogmec.go.jp/jogmec_db/map/php/login.php

Maus, S. and Dimri, V.P. (1996) Depth estimation from the scaling power spectrum of potential fields?, Geophys. J. Int., 124, 113-120.

National Renewable Energy Laboratory (2018) Geothermal Resources of the United States.

Newson, J., Mannington, W., Sepulveda, F., Lane, R. G., Clearwater, E., & O’Sullivan, M. J. (2012). Application of 3D Modelling and Visualization Software To Reservoir Simulation: Leapfrog Geothermal and Tough2. Proceedings of Thirty Seventh Workshop on Geothermal Reservoir Engineering, 6.

Okubo, Y., Makino, M. and Kasuga, S. (1991) Magnetic model of the subduction zone in the northeast Japan Arc, Tectonophysics, 192, 103-115.

Okubo, Y., Tsu, H. and Ogawa, K. (1989) Estimation of Curie point temperature and geothermal structure of island arcs of Japan, Tectonophysics, 159, 279-290.

Okubo, Y., Yamano, S., Takanashi, K., Akazawa, S., Osato, K. and Terai, A. (2023) Constraining the geotherm beneath the Japanese islands from Curie point depth analysis and comparison with seismicity and drillhole data in the Kakkonda geothermal field. Geothermics, **111**, 102706.

Spector, A. and Grant, S. (1970) Statistical models for interpreting aeromagnetic data, Geophysics, 35, 293–302.

Taylor, P. (2014) Supercritical carbon dioxide geothermal energy system analysis, University of Southern Queensland Faculty of Engineering and Surveying.